Materials Science, Vol. 43, No. 3, 2007

NANOTECHNOLOGY-ASSOCIATED COATINGS FOR AIRCRAFTS

R. Asmatulu,[1] R. O. Claus,[2,3] J. B. Mecham,[3] and S. G. Corcoran[4]

Polymeric epoxy-based composites are modified with nanopowders of silicon oxide (~100 nm). By the method of spraying, these composites are applied to specimens of 2024-T3 aluminum alloy preliminary treated with molybdate solutions to get conversion layers. Three types of polymeric coatings are considered: reference, treated by silica, and with additional polyurethane coatings. The aim of modification of polymeric coatings is to absorb and/or block unwanted ions/molecules (Cl^-, O_2, OH^-, H_2O, etc.) and improve the protective properties of the films. The tests carried out by the method of electrochemical impedance spectroscopy, in a salt-fog chamber, and by immersion in a 0.5 M NaCl solution reveal high anticorrosion characteristics of the coating. New coatings are promising for the corrosion protection in the aircraft industry.

Introduction

Corrosion is a phenomenon of deteriorating materials or their surfaces due to the environmental influences (chemical, physical, and physicochemical). Surface passivation and organic thin-film coatings seem to be the important means of protecting materials from corrosion attack. However, corrosion attack can still take place in the long term causing huge economical, safety, and environmental concerns. It is estimated that approximately 5% of an industrialized nation's gross national product (GNP) is spent for corrosion prevention, replacement of corroded parts, maintenance, and environmental protection. This corresponds to a cost of about $280 billion to the U.S. economy per year at the 2003 prices [1–6].

Protective coatings are probably the most widely accepted system for corrosion control. Therefore, thin-film coatings are frequently utilized to protect metal surfaces against corrosion attack. These organic films, such as polyurethane, polyamide, polyester, and epoxy play a crucial role as a barrier layer to reduce the transport of corrosive species when these species interact with the interfaces. Corrosion prevention also depends on the polarization and pores of the coating material and its capacitance that can be adjusted by the organic films on the metal surface. The atmospheric influence on a metal with organic coatings results in cracking, chalking, blistering, delamination, buckling, spalling, and colour changes, as well as in the corrosion formation on the metal surface [1–7].

In addition to these, the methods of surface treatment are used to reduce corrosion formation and thereby adhesion between the metal and coating materials [16, 20, 21]. For these purposes, hexavalent chromate, zinc, and phosphate-based materials are employed to increase the corrosion resistance of the surfaces and the quality of the coating [8–10]. However, it is reported that some of these materials (e.g., Cr) might not be ecologically friendly and, hence, alternative systems may be considered to reduce the environmental concerns. Recently,

[1] Department of Mechanical Engineering, Wichita State University, Wichita, USA.

[2] Fiber & Electro Optics Research Center, Virginia Tech., Blacksburg, USA.

[3] NanoSonic Inc., Blacksburg, USA.

[4] Department of Materials Science and Engineering, Virginia Tech., Blacksburg, USA.

Published in Fizyko-Khimichna Mekhanika Materialiv, Vol. 43, No. 3, pp. 103–108, May–June, 2007. Original article submitted May 21, 2007.

several research programs have been focused on low-toxicity surface treatment materials that may replace currently used ones [8, 21, 22].

In the present study, experiments were conducted on Al-alloy (2024-T3) substrates modified by molybdenum, epoxy coating, nanocomposites coating, and urethane top coating to analyze possible corrosion mitigating effects.

Experimental

Materials. An Al-alloy substrate (2024-T3) [Cu (3.8–4.9%), Cr (0.1%), Fe (0.5%), Mg (1.2–1.8%), Mn (0.3–0.9%), Si (0.5%), Ti (0.15%), Zn (0.25%), and other elements (0.15%); balance Al] commonly used in the aircraft industry was chosen for testing [24]. After removing the nylon covers on Al substrates, the samples $(1 \times 2.5 \times 7.5\ \text{cm})$ were degreased in acetone and 2-propanol (isopropyl alcohol) with 5 min of sonication before use. They were then all treated with a sodium molybdate dehydrate (Dow Chemical) for the conversion coating, which is more environmentally friendly surface coating method [1–4]. In this procedure, 5.57 g of sodium molybdate dehydrate was dissolved in 250 g of DI water (Barnstead Nanopure Water System) adjusted to pH 4 by using phosphoric acid (Aldrich). The degreased samples were immersed in this Mo solution for 20 min. After extraction from the solution, excess molybdate was removed with a rubber blade. The samples were washed truly with DI water.

The Mo-treated substrates were split into three groups. By using an air nozzle spray, these three groups of prepared substrates were coated with three different coating systems of variable thickness. The first group was coated with an acrylic-based epoxy (Dow Chemicals) with a thickness of 76.2 μm. This group is referred to as the "epoxy-coated" group. The second group was coated with the same acrylic-based epoxy mixed with 10% positively charged porous silica particles (~ 100 nm) (Silojet 703C) of the same thickness. This group is referred to as the "nanocomposite coating" group. The final set of prepared substrates was coated with the same nanocomposite coating with a thickness of 50.8 μm, which was then covered with a 25.4-μm-thick urethane (Dow Chemicals) top coating. In order to prepare the nanocomposite coating materials, the stabilized silica nanoparticles in a solution were added to the epoxy and then mixed for 30 min at high speed prior to air-nozzle spraying. Every test was repeated three times and the results were averaged.

Methods. Electrochemical Impedance Spectroscopy (EIS), salt spray (Q Fog Salt Spray), and salt soaking tests were carried out on the prepared samples to investigate their corrosion behavior in a 0.5 M NaCl (Fisher) solution. For the EIS tests, the prepared salt solution was replaced with a newly prepared solution every week. The EIS experiments were conducted by using both an EG&G PARC-273 potentiostat and a Gamry potentiostat (Model PC4/750) driven by the Zplot software. A 10 mV potential amplitude was applied to the electrode in the frequency range 0.1–100,000 Hz. This potential is fairly low (below the breakdown voltage) to avoid any damage to the film surface. The impedance data were collected at the open-circuit potential on specimens held in the 0.5 M NaCl solution for various periods of time. It is expected that the EIS scans of the coated specimens give higher values of electric resistance (R_c) and lower values of capacitance (C_c) than for the uncoated specimens in view of the lower dielectric properties of the organic coating materials.

In the EIS studies, the samples were immersed in the salt solution for a desired period of time, removed from the container, and mounted on an EG&G Princeton Applied Research Model K0235 Flat Cell with an area of the working electrode of 1 cm^2. The flat cell consists of a flat cylinder horizontally clamped between two end plates. One end of the plate houses the working electrode and the other is the platinum counter electrode. A mercury/mercurous-sulfate reference electrode was used in a Luggin well. During the tests, thick polymeric tapes covered the uncoated backsides of the substrates to be able to avoid experimental errors. The EIS data

were analyzed by using a fitting program called ZsimpWin, which basically fits the experimental impedance data received from EIS measurements to the electronic-circuit models. The modulus of the impedance as a function of frequency was obtained for each set of samples after various times of holding in the 0.5 M NaCl solution. It is known that low-frequency impedance values (Z_f) measure barrier and transport properties for coated substrates held in aggressive salt solutions [1–4]. The impedance modulus $|Z|$ corresponding to 5 mHz (low-frequency domain) were calculated and compared with each other.

The standard salt-spray test was used for the corrosion experiments [27]. In the present tests, the salt spray tests were conducted on the coated substrates by using a Q.FOG cyclic corrosion tester. The coated substrates were placed into the 0.5 M aqueous-salt fog atmosphere in the spray machine for two time periods, 168 and 336 h at 35°C, 1 kg/cm^2 of pressure and neutral pH. The salt solution was prepared by using filtered water. Every 24 h, the samples were removed from the salt-spray machine to take pictures, and then the results were visually evaluated for each sample.

Salt-soaking tests were conducted by completely immersing coated samples in a glass container with a 0.5 M NaCl solution for 90 days at room temperature. After this time period, the samples were removed from the containers, photographed, and visually evaluated for comparison.

Results and Discussion

EIS Studies. *Mo Treatment.* The results of the EIS tests (Fig. 1a) indicate that the molybdenum treatment reveals a low coating resistance for the first 15 days of holding in the 0.5 M NaCl solution, which then decreases to lower levels beyond that period of time. This may be attributed to the fact that, after a certain period of time, the resistance of the molybdenum coating against the corrosive ion attack in the NaCl solution may be lost. In the absence of the Mo conversion coating, the surface resistance of freshly peeled Al substrates was closer to zero.

Epoxy Coating. The coating resistance of samples is approximately equal to $10^5\,\Omega\cdot\text{cm}^2$ in the early stages of the immersion time (Fig. 1b). As the test progresses, its values show an exponential decrease. This may be due to the fact that chlorine, oxygen, and hydroxyl ions and water molecules penetrate through the thin films on the substrates, thus weakening the coating resistance. However, the coating resistance of these samples is still higher, by an order of magnitude, than for the Mo passivated surface after 40 days of holding.

Nanocomposite Coating. There were no adhesive failures (delamination, buckling, or spalling) between the substrates and the coatings and no cohesive failure (microcracking) on the coating materials [1–3, 23]. The corrosion resistance of the nanocomposite coatings was over $10^6\,\Omega\cdot\text{cm}^2$ (Fig. 1c) during the first day of holding in the salt solution. However, after 40 days of immersion, the resistance gradually decreased to $3\times10^4\,\Omega\cdot\text{cm}^2$. This represents higher corrosion resistances than for the acrylic-based epoxy coating in the early period (first ten days) of immersion. After this, the electrolytic solution possibly reached the interface and degraded the properties of the coating (its resistance, capacitance, dielectric properties, etc.) [17–19]. The higher coating resistance may be due to the fact that the positively charged porous silica particles absorb and/or block unwanted species (e.g., Cl^-, O_2, H_2O, etc.). It was also seen that, in some tests, the coating resistance first decreased and then increased during the period of holding. This can be explained by the blockage of the pores in the coating materials over that particular time period. In the future studies, we will seriously consider this approach.

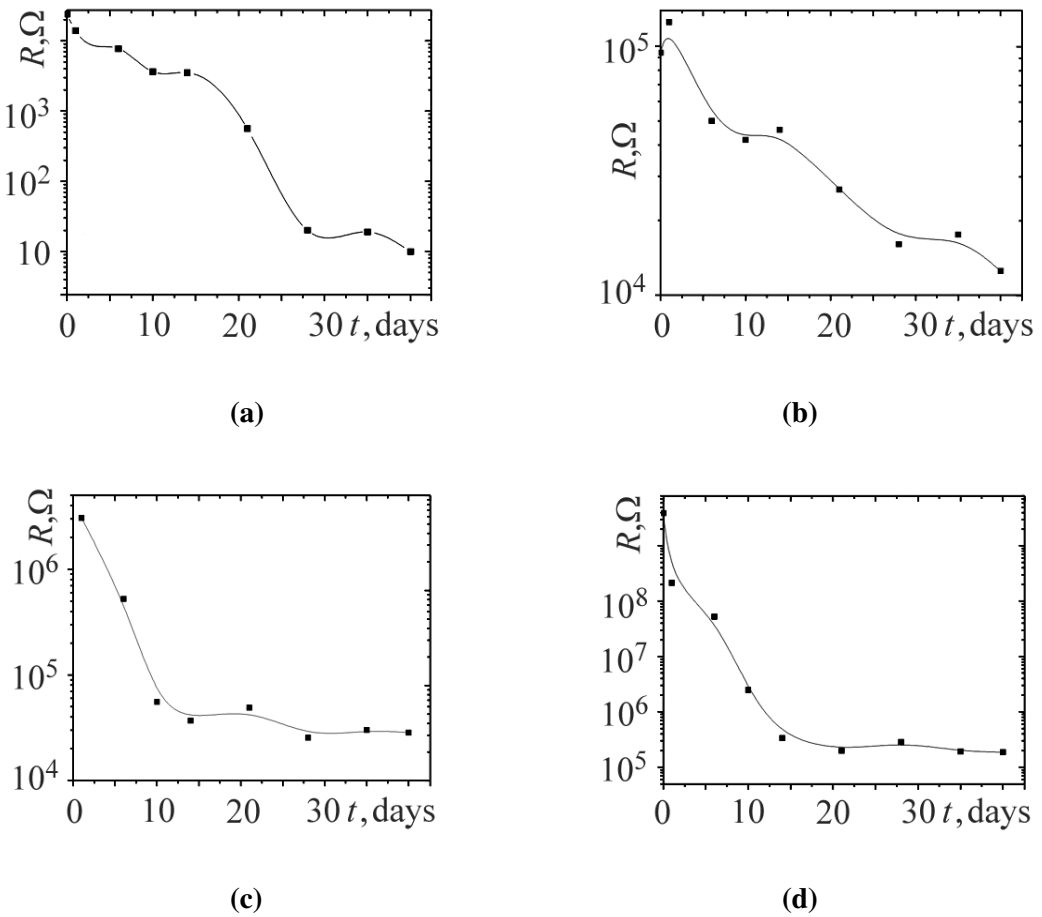

Fig. 1. Total coating resistance R of: (a) sodium molybdate dehydrate surface treatment, (b) epoxy films, (c) nanocomposite thin films, (d) nanocomposite thin films with urethane coating on 2024-T3 Al substrates as a function of the time of holding in 0.5 M NaCl solutions at room temperature.

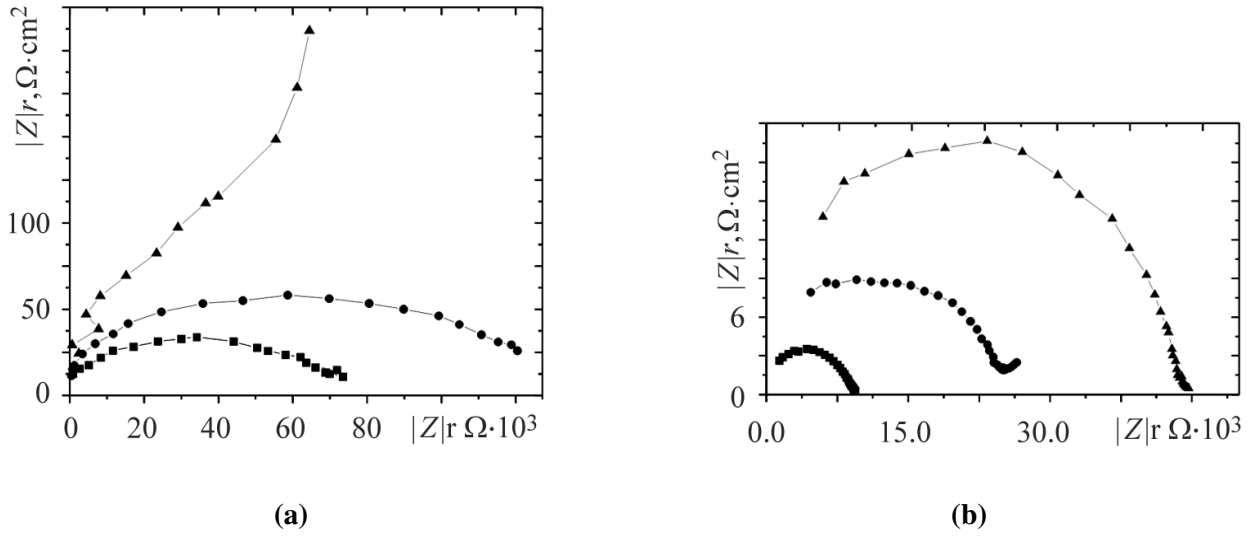

Fig. 2. Nyquist plots of the coated 2024-T3 Al samples for the first day (a) and the 40th day (b) of holding in the 0.5M NaCl solution at room temperature: (■) epoxy coating, (●) nanocomposite coating, (▲) nanocomposite with urethane.

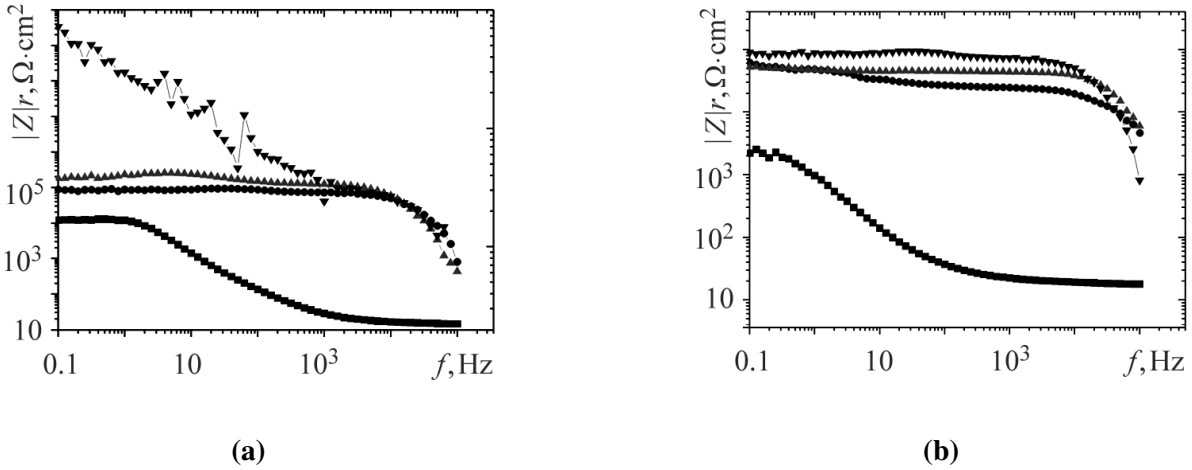

(a) **(b)**

Fig. 3. Bode plots of the treated 2024-T3 Al samples for the first day (a) and the 40th (b) day of holding as functions of frequency (Hz) in the 0.5M NaCl solution at room temperature: (■) Mo treatment, (●) epoxy coating, (▲) nanocomposite coating, (▼) nanocomposite with urethane.

Nanocomposite with Urethane Top Coating. Urethane is a favorable coating material with a wide variety of osmotic barrier, chemical, thermal, hydrolytic, and oxidative stability properties that can be advantageous for corrosion prevention [1–3, 16] (Fig. 1d). However, the cost of urethane is a lot higher than the cost of conventional organic coatings and, hence, it is mostly utilized as the second layer. Thus, one of the main goals of this experiment is to lower the amount of urethane coating in the system using the nanocomposite coating. As can be seen, these novel samples provided the total coating resistance over $10^9\,\Omega \cdot cm^2$ (Mo surface and nanocomposite with urethane top layer) in the first day of holding and then gradually degraded. In the initial stage, this coating resistance is approximately six, five, and four orders of magnitudes higher than for the Mo conversion coating, the epoxy coating, and the nanocomposite coating, respectively. This barrier effect can be attributed to the absorption/blockage of unwanted ions or molecules by the nanosize porous silica particles and the high corrosion resistance of urethane [12–18]. It is assumed that the indicated improvement continues until the coating substrates are completely saturated with these ions and molecules. The difference between the values of coating resistance for the first and tenth days steadily decreased and then remained quite constant for about 30 days. As a result, we conclude that the indicated high coating resistance can efficiently protect the aircraft surfaces against corrosion.

Analysis of the EIS Diagrams. The corrosion behaviors of the coated Al substrates were investigated by using the Nyquist (real impedance vs. imaginary impedance) and Bode (real impedance vs. frequency) plots for the first and 40th days of the period of immersion. The results clearly demonstrate that the nanocomposite with urethane top coating has the greatest corrosion performance at the beginning of the immersion time (Fig. 2a). As the immersion time extends to 40 days, all samples begin to lose their coating performance (Fig. 2b), which shows that there is some degree of degradation in the coating materials [16–22].

The dependence of imaginary resistance $|Z''|$ on frequency reveals that the urethane top-coated samples exhibit the highest values of real impedance $|Z''|_{\text{real}}$, while the Mo treated Al coupons give the lowest values (Fig. 3a). This is because the former sample presents the highest coating resistance in the 0.5 M NaCl solution due to the barrier effects of the coatings and do not degrade as much as the other samples. In general, it is believed that the modulus of real impedance $|Z''|_{\text{real}}$ decreases as the time of holding increases due to the loss of the protective properties of the coatings (Fig. 3b) [12–19].

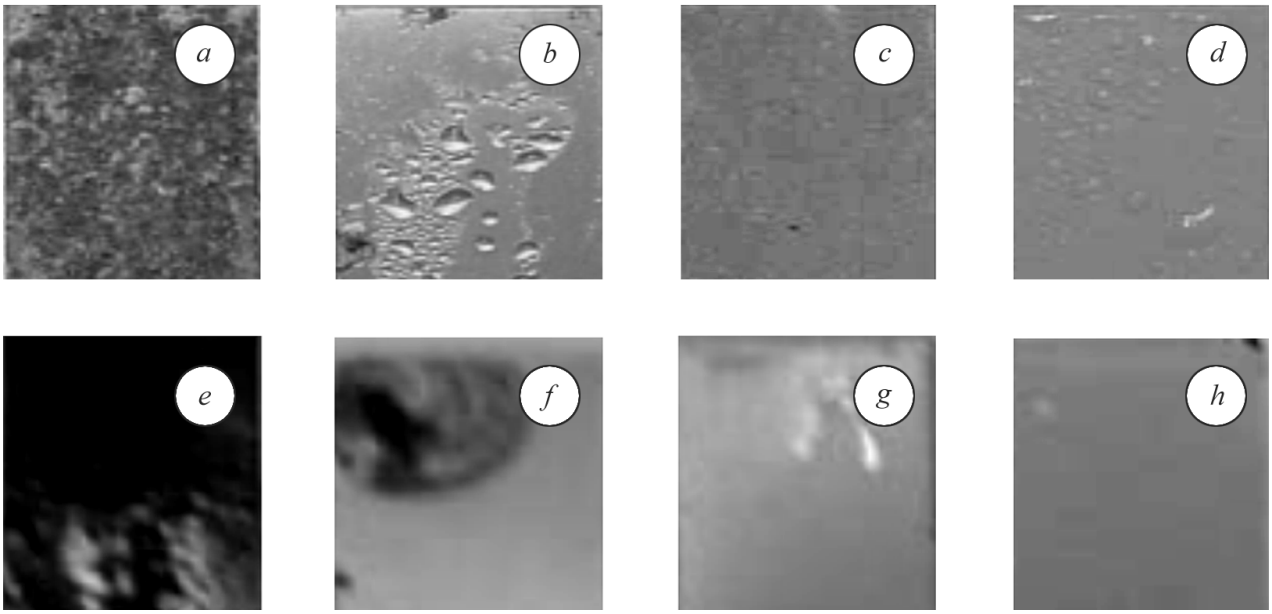

Fig. 4. Photographs of 2024-T3 Al substrates treated with: (a, e) Mo, (b, f) acrylic-based epoxy coating, (c, g) nanocomposite coating, (d, h) nanocomposite with urethane top coating; after 14 days (a–d) of 0.5M NaCl salt-spray atmosphere at 35°C and 1 kg/cm^2 and (e–h) after 90 days of 0.5M NaCl salt soaking at room temperature.

Salt Spray Tests. In the first and seventh (168 h) days of salt-spray tests, all samples appeared to be in good condition except the Mo-coated samples (Fig. 4a). The color of these samples changed from their original colors to gray. When the time of spraying increased to 14 days (336 h) (Fig. 4d), the nanocomposites with urethane top coating did not show significant blisters, holes, or color changes. Moreover, the epoxy coating (Fig. 4b) showed small blisters and a color change, while the nanocomposite coating (Fig. 4c) showed only a color change. Meanwhile, the surface of the Mo-coated samples (Fig. 4a) was severely corroded and exhibited the highest corrosion levels after 14 days of salt spraying. This could be explained by the higher rate of reaching of the interface between the solution and the metal surface by the electrolytic solution. These results are also in good agreement with the EIS test results. Further studies will extend the salt-spray testing to several weeks at higher temperatures and pressures to determine the coating properties of the materials.

Salt Soaking Tests. In these tests, samples from each test group were immersed in a 0.5 M NaCl solution for 90 days at room temperature. The Mo-coated samples (Fig. 4e) show severe damage and develop the highest corrosion rates. This might also be the result of penetration of the unwanted ions and molecules through the interface [17–20]. The epoxy-coated samples (Fig. 4f) showed a few edge blisters and color changes, while the nanocomposite-coated samples (Fig. 4g) showed only color changes. However, the urethane-top-coated samples (Fig. 4h) did not show significant central and/or edge blisters, holes, or colour changes and appeared to be in excellent conditions as compared to the other samples. In the future study, we will optimize the amount of urethane top coating in the system in order to reduce the overall coating cost.

CONCLUSIONS

Corrosion tests were conducted on 2024-T3 Al samples modified by Mo, epoxy coating, nanocomposite coating, and nanocomposite coating with the urethane top layer. The corrosion results obtained by using the EIS,

salt-spray and salt-soaking tests show that the Mo-treated Al surface gives the lowest corrosion resistance, while the nanocomposite with urethane top coating presents the highest coating resistance. This can possibly be explained by the barrier effect of positively charged nanosize porous silica particles and the urethane top coating. The present study may provide promising results for the corrosion prevention in the aircraft industry, as well as in many other industries.

REFERENCES

1. P. R. Roberge, *Handbook of Corrosion Engineering,* McGraw-Hill, New York (2000).
2. P. A. Schweitzer, *Atmospheric Degradation and Corrosion Control,* Marcel Dekker, New York (1999).
3. D. Jones, *Principles and Prevention of Corrosion,* 2nd edition, Prentice Hall, Upper Saddle River, NJ (1996).
4. C. Corfias, N. Pebere, and C. Lacabanne, "Characterization of a thin protective coating on galvanized steel by electrochemical impedance spectroscopy and a thermostimulated current method," *Corr. Sci.,* **41**, 1539–1555 (1999).
5. C. Corfias, N. Pebere, and C. Lacabanne, "Characterization of protective coatings by electrochemical impedance spectroscopy and a thermostimulated current method. Influence of the polymer binder," *Corr. Sci.,* **42**, 1337–1350 (2000).
6. J. O. Iroh and W. Su, "Corrosion performance of polypyrrole coating applied to low-carbon steel by an electrochemical process," *Electrochim. Acta,* **46**, 15–24 (2000).
7. R. J. Scully and S. T. Hensley, "Lifetime prediction for organic coatings on steel and a magnesium alloy using electrochemical impedance methods," *Corr. Sci.,* **50**, No. 9, 705–716 (1994).
8. L. Fedrizzi, F. J. Rodriguez, S. Rossi, F. Deflorian, R. Di Maggio, "The use of electrochemical techniques to study the corrosion behavior of organic coatings on steel pretreated with Sol-Gel Zirconia Films," *Electrochim. Acta,* **46**, 3715–3524 (2001).
9. L. Fedrizzi, A. Bianchi, F. Deflorian, S. Rossi, and P. L. Bonora, "Effect of chemical cleaning on the corrosion behavior of painted aluminum alloys," *Electrochim. Acta,* **47**, 2159–2168 (2002).
10. M. F. Montemor, A. M. Simoes, M. G. S. Ferreira, B. Williams, and H. Edwards, "The corrosion performance of organosilane based pretreatments for coatings on galvanized steel," *Progr. Org. Coat.,* **38**, 17–26 (2000).
11. L. Salanais, "Prevention of corrosion in aircraft—an overview of the evolution of materials and protective treatments," *CIM Bull.,* **81** (915), 103–110 (1988).
12. W. D. Callister, Jr., *Materials Science and Engineering. An Introduction,* 5th edition, Wiley, New York (2000).
13. W. S. Tait, K. A. Handrich, and S. W. Tait, "Analyzing and interpreting EIS data from internally coated steel aerosol containers," in: Scully, Silverman, and Kending (editors), *Electrochemical Impedance: Analysis and Int.,* ASTM STP 1188 (1993), pp. 428–437.
14. J. R. Scully, "Electrochemical impedance of organic coated steel: correlation of impedance parameters with long-term coating deterioration," *J. Electrochem. Soc. (JES),* **136**, No. 4, 979 (1989).
15. A. S. Hamdy, A. M. Baccaria, and T. Temtchenko, "Corrosion protection of AA6061 T6 by fluoropolymer coatings in NaCl solution," *Surf. Coat. Technol.,* **155**, 176–183 (2002).
16. R. Asmatulu and R. O. Claus, "Corrosion protection of materials surfaces by applying nanotechnology associated studies," in: *Mat. Res. Soc. Symp. Proc.* (MRS 2004 Spring Meeting, Boston), Vol. 788 (2004), pp. LI 1.44.1–L11.44.6.
17. J. M. Yeh, S. J. Liou, C. G. Lin, Y. P. Change, Y. H. Yu, and C. F. Cheng, "Effective enhancement of anticorrosion properties of polystyrene by polystyrene-clay nanocomposite materials," *J. Appl. Polymer Sci.,* **92**, 1970–1976 (2004).
18. V. J. Gelling, M. M. Weist, D. E. Tallman, G. P. Bierwagen, and G. G. Wallace, "Electroactive-conducting polymers for corrosion control. 4. Studies of poly(3-octyl)pyrrole and poly(3-octadecyl)pyrrole on aluminum 2024-T3 alloy," *Progr. Organ. Coat.,* **43**, 149–157 (2001).
19. Q. L. Thu, G. P. Bierwagen, and S. Touzain, "EIS and ENM measurements for three different organic coatings on aluminum," *Progr. Organ. Coat.,* **42**, 179–187 (2001).
20. T. L. Metroke, O. Kachurian, and E. T. Knobbe, "Spectroscopic and corrosion resistance characterization of GLYMO-TEOS ormosil coating for aluminum alloy corrosion inhibition," *Progr. Organ. Coat.,* **44**, No. 202, 295–305.
21. D. Chidambaram, M. J. Vasquez, G. P. Halada, and C. R. Clayton, "Studies on the repassivation behavior of aluminum and aluminum alloy exposed to chromate solutions," *Surf. Interf. Anal.,* **35**, 226–230 (2003).
22. L. De Rosa, T. Monetta, F. Bellucci, D. B. Mitton, A. Atienza, and C. Sinagra, "The effect of a conversion layer and organic coating on the electrochemical behavior of 8006 and 8079 aluminum alloys," *Progr. Organ. Coat.,* **44**, 153–160 (2002).

23. R. Asmatulu, R. O. Claus, and I. Tuzcu, "Adhesion failure of thin-film coatings by internal and external stresses at interfaces," in: *Proc. of the Fifth Internat. Congr. on Thermal Stresses and Related Topics, TS2003 (June 2003, Blacksburg)* Blacksburg, VA (2003), pp. MA-6-3-1–MA-6-3-4.
24. http://www.lasurface.com/w_month_subj/ECASIA2001/Adsorption}%20of%20organic%20acids.pdf.
25. G. Grundmeier, W. Schmidt, and M. Stratmann, "Corrosion protection by organic coatings: electrochemical mechanism and novel methods of investigation," *Electrochem. Acta,* **45**, 2515–2533 (2000).
26. C. S. Kumar, V. S. Rao, V. S. Raja, A. K. Sharma, and S. M. Mayanna, "Corrosion behavior of solar reflector coatings on AA 2024T3—an electrochemical impedance spectroscopy study," *Corr. Sci.,* **44**, 387–393 (2002).
27. *ASTM B117: Standard Practice for Operating Salt Spray (Fog) Apparatus,* ASTM International (1997 Edition).